

# Journal of Computational and Nonlinear Dynamics

Published Quarterly by ASME

VOLUME 3 • NUMBER 2 • APRIL 2008

*SPECIAL ISSUE ON DISCONTINUOUS AND FRACTIONAL  
DYNAMICAL SYSTEMS*

## EDITORIAL

020201 Special Issue on "Discontinuous and Fractional Dynamical Systems"  
J. Tenreiro Machado and Albert Luo

## RESEARCH PAPERS

### Mathematical Theory

021101 Initialization of Fractional-Order Operators and Fractional Differential  
Equations  
Carl F. Lorenzo and Tom T. Hartley

021102 Fractional Constrained Systems and Caputo Derivatives  
Dumitru Baleanu

021103 Application of Incomplete Gamma Functions to the Initialization of  
Fractional-Order Systems  
Tom T. Hartley and Carl F. Lorenzo

021104 On the Differential Geometry of Flows in Nonlinear Dynamical Systems  
Albert C. J. Luo

### Modeling

021201 Fractional Dynamics: A Statistical Perspective  
J. A. Tenreiro Machado and Alexandra Galhano

021202 Formulation of A State Equation Including Fractional-Order State  
Vectors  
Masaharu Kuroda

021203 Fractional Dynamics in Mechanical Manipulation  
Miguel F. M. Lima, J. A. Tenreiro Machado, and  
Manuel Crisóstomo

021204 Fractional Optimal Control of a Distributed System Using  
Eigenfunctions  
Om P. Agrawal

021205 Dynamics of a Duffing Oscillator With Two Time Delays in Feedback  
Control Under Narrow-Band Random Excitation  
Yanfei Jin and Haiyan Hu

021206 Nonlinear Analysis of Road Traffic Flows in Discrete Dynamical  
System  
Meng Xu and Ziyong Gao

021207 Identifying a Transfer Function From a Frequency Response  
Duarte Valério, Manuel Duarte Ortigueira, and José Sá da Costa

### Implementation

021301 Microelectronic Implementations of Fractional-Order Integrodifferential  
Operators

Guillermo E. Santamaría, José V. Valverde, Raquel Pérez-Aloe, and  
Blas M. Vinagre

(Contents continued on inside back cover)

Editor  
SUBHASH C. SINHA (2010)

Associate Editors  
OM P. AGRAWAL (2008)  
KURT ANDERSON (2008)  
OLIVIER BAUCHAU (2008)  
B. BALACHANDRAN (2008)  
ALAIN BERLIOZ (2008)  
HARRY DANKOWICZ (2008)  
AL FERRI (2008)  
HENRYK FLASHNER (2010)  
DAVID E. GILSINN (2009)  
CLAUDE-HENRI LAMARQUE (2009)  
HAMID LANKARANI (2008)  
ALBERT C. J. LUO (2009)  
JOHN MCPHEE (2008)  
AKI MIKKOLA (2009)  
FRIEDRICH PFEIFFER (2008)  
CHRISTOPHER PIERRE (2008)  
GIUSEPPE REGA (2008)  
WERNER SCHIEHLEN (2008)  
AHMED SHABANA (2008)  
NOBUYUKI SHIMIZU (2009)  
ANAND V. SINGH (2008)  
LAWRENCE VIRGIN (2008)  
WAN-SUK YOO (2009)

PUBLICATIONS COMMITTEE  
Chair, BAHRAM RAVANI

OFFICERS OF THE ASME  
President, SAM Y. ZAMRIK  
Executive Director, VIRGIL R. CARTER  
Treasurer, THOMAS D. PESTORIUS

PUBLISHING STAFF  
Managing Director, Publishing  
PHILIP DI VIETRO  
Manager, Journals  
COLIN MCATEER  
Production Coordinator  
TARA SMITH

Transactions of the ASME, Journal of Computational  
and Nonlinear Dynamics (ISSN 1555-1423) is published  
quarterly (January, April, July, October) by The American  
Society of Mechanical Engineers, Three Park Avenue,  
New York, NY 10016-5990.

POSTMASTER: Send address changes to Transactions of the  
ASME, Journal of Computational and Nonlinear Dynamics, c/o  
THE AMERICAN SOCIETY OF MECHANICAL ENGINEERS,  
22 Law Drive, Box 2300, Fairfield, NJ 07007-2300.

CHANGES OF ADDRESS must be received at Society  
headquarters seven weeks before they are to be effective.  
Please send old label and new address.

STATEMENT from By-Laws. The Society shall not be  
responsible for statements or opinions advanced in papers  
or ... printed in its publications (B7.1, Para. 31).

COPYRIGHT © 2008 by The American Society of Mechanical  
Engineers. For authorization to photocopy  
material for internal or personal use under those  
circumstances not falling within the fair use provisions  
of the Copyright Act, contact permissions@asme.org.

REPRINTS: Requests for reprints should be addressed  
to Marisol Andino, andinom@asme.org.

Canadian Goods & Services Tax Registration #126148048

CONTACT THE EDITOR: Professor S.C. Sinha,

Department of Mechanical Engineering, 202 Rose Hall,  
Auburn University, Auburn, AL 36849

T: 334-844-3325

F: 334-844-3307

E: ssinha@eng.auburn.edu

This journal is printed on acid-free paper, which exceeds the ANSI Z39.48-

1992 specification for permanence of paper and library materials. ©™

85% recycled content, including 10% post-consumer fibers.

*Special Issue on Discontinuous and Fractional Dynamical Systems*

**JOURNAL  
OF  
COMPUTATIONAL  
AND  
NONLINEAR  
DYNAMICS**

# FRACTIONAL DYNAMICS IN MECHANICAL MANIPULATION (DETC2007-35418)

**Miguel F. M. Lima\***

Dept. of Electrical Engineering  
Superior School of Technology  
Polytechnic Institute of Viseu  
3504-510 Viseu, Portugal  
*lima@mail.estv.ipv.pt*

**J.A. Tenreiro Machado**

Dept. of Electrical Engineering  
Institute of Engineering  
Polytechnic Institute of Porto  
4200-072 Porto, Portugal  
*jtm@isep.ipp.pt*

**Manuel Crisóstomo**

Institute of Systems and Robotics  
Dept. of Electrical and Computer Engineering  
University of Coimbra, Polo II  
3030-290 Coimbra, Portugal  
*mcris@isr.uc.pt*

## ABSTRACT

This paper analyzes the signals captured during the movement of a mechanical manipulator carrying a liquid container. In order to study the signals an experimental setup is implemented. The system acquires data from the sensors, in real time, and, in a second phase, processes them through an analysis package. The analysis package runs off-line and handles the recorded data. The results show that the Fourier spectrum of several signals presents a fractional behavior. The experimental study provides useful information that can assist in the design of a control system to be used in reducing or eliminating the effect of vibrations.

## INTRODUCTION

In practice the robotic manipulators present some degree of unwanted vibrations. In fact, the advent of lightweight arm manipulators, mainly in the aerospace industry, where weight is an important issue, leads to the problem of intense vibrations. On the other hand, robots interacting with the environment often generate impacts that propagate through the mechanical structure and produce also vibrations.

Motivated by the problem of vibrations, this paper studies the robotic signals captured during the motion of a spherical container attached to the manipulator. The container carries a liquid and its acceleration induces motion of the content causing consequently a liquid vibration. The study is done in a fractional calculus (FC) perspective. In order to analyze the phenomena involved an acquisition system was developed. The manipulator motion produces vibrations, either from the structural modes or from the liquid vibration. The instrumentation system acquires signals from multiple sensors that capture the axis positions, mass accelerations, forces and moments and electrical currents in the motors. Afterwards, the analysis package, running off-line, reads the data recorded by the acquisition system and examines them.

Bearing these ideas in mind, this paper is organized as follows. Section 2 addresses the motivation for this work. Section 3 describes briefly the robotic system enhanced with the instrumentation setup. Section 4 presents the experimental

results. Finally, section 5 draws the main conclusions and points out future work.

## MOTIVATION

Singer and Seering [1] mention several techniques for reducing vibrations and its implementation either at the robot manufacturing stage or at the operational stage. Briefly, the techniques can be enumerate as: (i) conventional compensation, (ii) structural damping or passive vibration absorption, (iii) control based on the direct measurement of the absolute position of the gripper, (iv) control schemes using the direct measurement of the modal response, (v) control driving, actively, energy out of the vibration modes, (vi) use a micromanipulator at the endpoint of the larger manipulator and (vii) adjustment of the manipulator command inputs so that vibrations are reduced or eliminated.

In recent years the study of micro/macro robotic manipulators has been receiving considerable attention. In fact, this approach was employed in manipulators that have been proposed for space applications and nuclear waste cleanup. Several authors studied this technique, namely Magee, *et al.* [3] and Cannon, *et al.* [4] that adopted the command filtering approach in order to position the micromanipulator. Also, Cannon, *et al.* [4] and Lew, *et al.* [5] used inertial damping techniques taking advantage of a micro manipulator located at the end of a flexible link. Yoshikawa, *et al.* [2] used the redundancy of a flexible macro-micro manipulator system to generate the joint trajectories in order to reduce the effect of vibration at the end-effector.

One of the applications where the vibration occurs is in the manipulation of liquids. Here there are two main aspects: the modeling and the control of the liquid dynamics. Several authors addressed the dynamics problem due to liquid slosh loads. There are several mathematical tools to describe the fluids. For example, Navier-Stokes equations [16] can be used to model the liquid dynamics. Concerning the problem of control the liquid vibration, it was first encountered in control of guided missiles in the aerospace industry. In this application it was found that sloshing in the fuel tanks could result in instabilities. Lately, movement of open containers

\* Author of correspondence, Phone: (+351) 232 480 627, Fax: (+351) 232 424 651

containing fluid, e.g. molten metal and various beverages, has been investigated. The main goal is then to move the container as fast as possible without too much slosh [16, 17].

Bearing these ideas in mind, this article studies the robotic signals in a FC perspective. In fact, the study of fractional order systems has been receiving considerable attention [6, 7, 22–25] due to the facts that many physical systems are well characterized by fractional models [8]. With the success in the synthesis of real noninteger differentiators, the emergence of new electrical elements [9], and the design of fractional controllers [10], fractional algorithms have been applied in a variety of dynamical processes [11]. Therefore, the study presented here can assist in the design of the control system to be used.

### EXPERIMENTAL PLATFORM

The developed experimental platform has two main parts: the hardware and the software components [12]. The hardware architecture is shown in figure 1. Essentially it is made up of a robot manipulator, a Personal Computer (PC) and an interface electronic system. The interface box is inserted between the robot arm and the robot controller, in order to acquire the internal robot signals; nevertheless, the interface captures also external signals, such as those arising from accelerometers and force/torque sensors, and controls the external micro-arm. The modules are made up of electronic cards specifically designed for this work. The function of the modules is to adapt the signals and to isolate galvanically the robot's electronic equipment from the rest of the hardware required by the experiments.

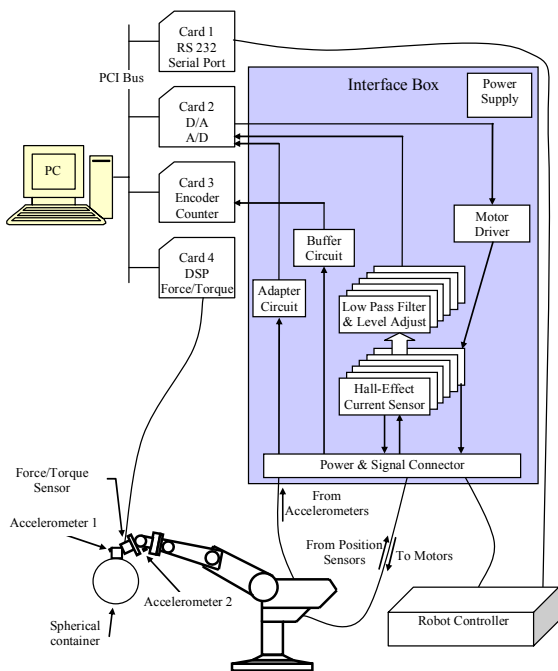


Figure 1. Block diagram of hardware architecture

The software package runs in a Pentium 4, 3.0 GHz PC and, from the user's point of view, consists on two applications: the acquisition application and the analysis

package. The acquisition application is a real time program for acquiring and recording the robot signals. The analysis package runs off-line and handles the recorded data. This program allows several signal processing algorithms such as, Fourier transform (FT), correlation, time synchronization, etc.

### EXPERIMENTAL RESULTS

In the experiment is adopted a spherical container. Its physical properties are shown in Table 1. To test the behavior of the variables in different situations, the container can remains empty or its content can be a liquid or a solid. Figure 2 depicts the robot with the container. The robot motion is programmed in a way that the container moves from an initial to a final position following a linear trajectory. The distance between the points is 0.6 m.



Figure 2. Spherical container with liquid

Table 1 – Physical properties of the spherical container

Characteristic	Spherical container
Mass (empty) [kg]	$215 \times 10^{-3}$
Diameter [m]	$203 \times 10^{-3}$

During the motion of the manipulator the container is moved by the robot and several signals are recorded with a sampling frequency of  $f_s = 500$  Hz. The signals come from different sensors, such as accelerometers, force and torque sensor, position encoders and current sensors. The signals are captured for three different situations: (i) empty container, (ii) container with a solid, and (iii) container with a liquid. The container with the solid or the liquid have an identical mass, namely of 1 kg. In the experiment the used liquid is water. The acceleration of the container induces motion of the liquid. This is referred to as slosh or liquid vibration. The amount of slosh depends on how the container is accelerated, the geometry of the container and the properties of the fluid.

In order to test different acceleration shapes two types of trajectory velocity are used: the trapezoidal and the parabolic profiles. The trapezoidal profile causes the motors to accelerate and decelerate quickly at the start and end of movement, with a constant speed along the path. The parabolic profile causes the motors to accelerate slowly, until maximum speed is reached, and then decelerate at the same rate.

**Time Domain:**

The time evolution of the variables is shown in the figures 3–12 corresponding to the cases: (i) empty container, (ii) container with a solid, and (iii) container with a liquid.

To analyze the vibration effect of the liquid, caused by the container acceleration, the signals are captured during 20 s, although the motion of the container is executed in approximately 5 s.

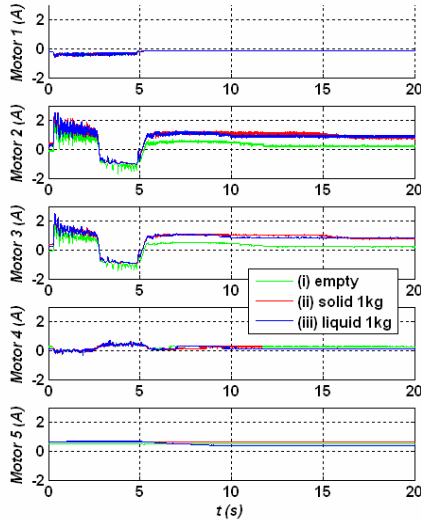


Figure 3. Electrical currents of robot axis motors for the trapezoidal profile

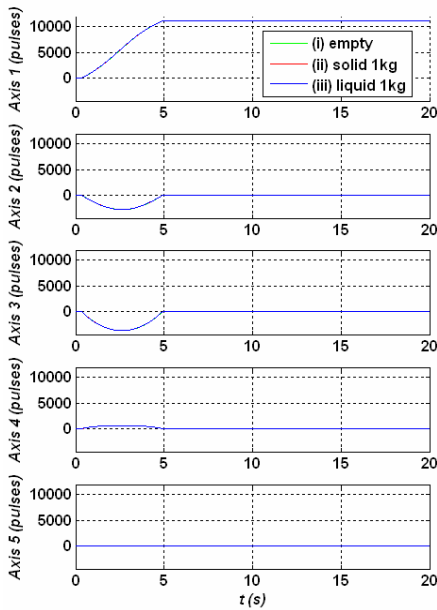


Figure 4. Robot axis positions for the trapezoidal profile

Figure 3 represents the electrical current of the motors for the trapezoidal profile. As consequence the robot joints rotate as shown in figure 4. The signals of axis 1 to 4 present a variation approximately during the first 5 s, that is the time

duration of the trajectory. According to the defined trajectory the axis 5 does not rotate.

Figures 5 and 6 show the forces and moments respectively in consequence of the container motion. The effect of the liquid vibration can be observed in the  $M_y$  moment component (figure 6).

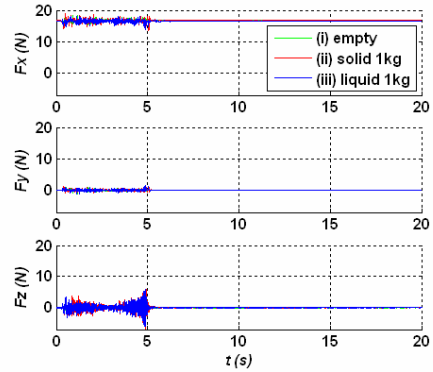


Figure 5. Forces at the gripper sensor for the trapezoidal profile

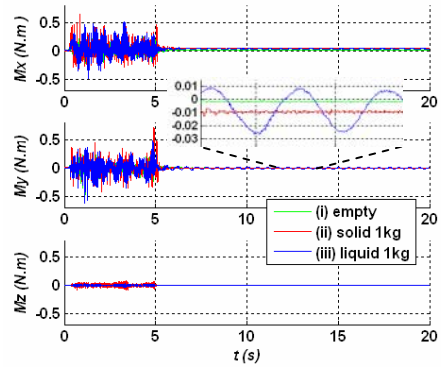


Figure 6. Moments at the gripper sensor for the trapezoidal profile

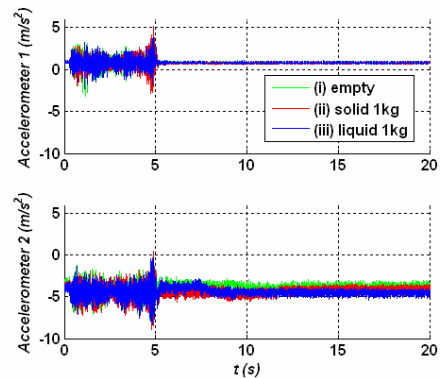


Figure 7. Container and terminal robot link accelerations for the trapezoidal profile

Figure 7 shows the accelerations at the clamped end of the container (accelerometer 1) and at the terminal link of the robot (accelerometer 2). The amplitudes of the accelerometers signals are higher at the end of the container movement.

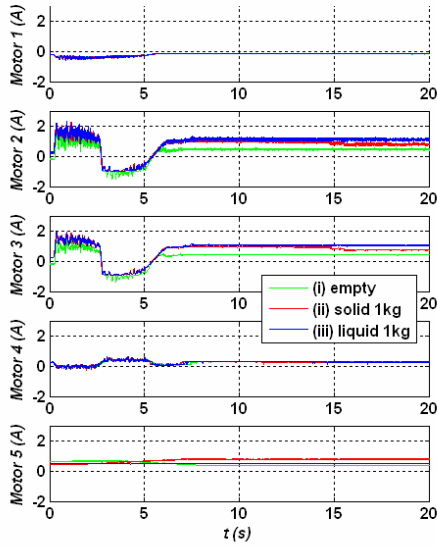


Figure 8. Electrical currents of robot axis motors for the parabolic profile

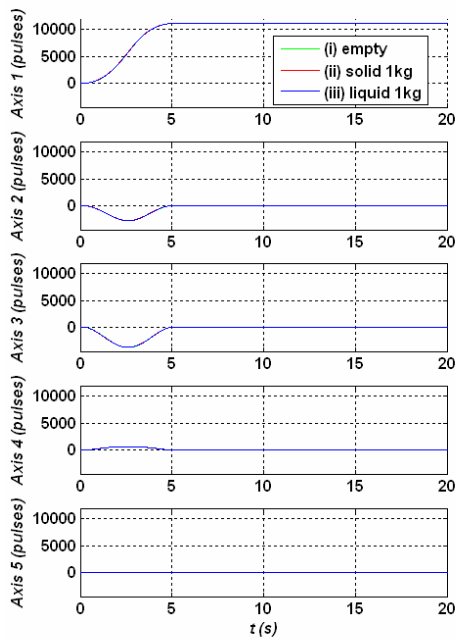


Figure 9. Robot axis positions for the parabolic profile

Figures 8-12 show the time evolution of the variables for the parabolic profile. Comparing the robot axis positions for the two profiles (figures 4 and 9) it can be seen that the dynamics of the signal positions at the start and end of movement are smoother for the parabolic case. This fact is also reflected in the electrical currents of the robot axis motors (figures 3 and 8).

The smoother dynamics of the parabolic profile has the consequence of lower forces induced in the container. Therefore, the amplitude of the liquid vibration, caused by the movement of the container, is lower than the acceleration

occurring in the trapezoidal case. This fact is reflected in the moments measured at the gripper sensor (see the zoom in figures 6 and 11). Also, for the trapezoidal profile the accelerations are higher at the end of trajectory, approximately at  $t = 5$  s (see figures 7 and 12).

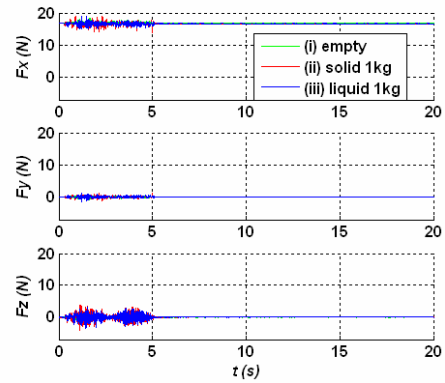


Figure 10. Forces at the gripper sensor for the parabolic profile

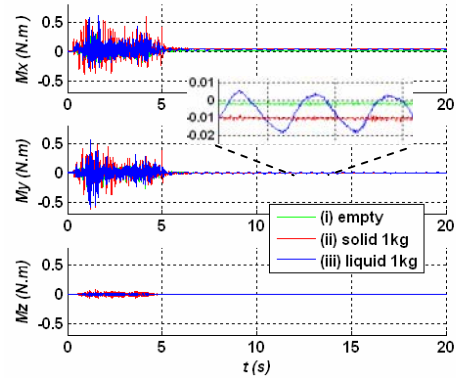


Figure 11. Moments at the gripper sensor for the parabolic profile

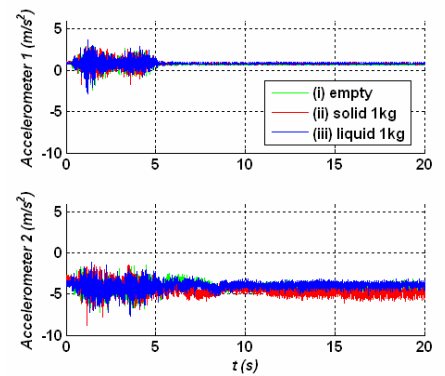


Figure 12. Container and terminal robot link accelerations for the parabolic profile

#### Fourier Transform:

In order to examine the behavior of the signal FT a trendline is superimposed within the spectrum over, at least,

one decade. The trendline is based on a power law approximation [14]:

$$|\mathcal{F}\{f(t)\}| \approx c\omega^m \quad (1)$$

where  $\mathcal{F}$  is the Fourier operator,  $c \in \mathbb{R}^+$  is a constant that depends on the amplitude,  $\omega$  is the frequency and  $m \in \mathbb{R}$  is the slope.

All the signals of the trajectories referred previously were studied but, due to space limitations, only the most relevant are depicted.

Figure 13 shows the amplitude of the Fast Fourier Transform (FFT) of the axis 1 position signal (case *i*). A trendline is calculated, and superimposed over the signal, with slope  $m = -0.99$ , that reveals, clearly, the integer order behavior. The position signals present identical behavior, in terms of its spectrum, for the others cases (*ii*) container with a solid and (*iii*) container with a liquid. In fact, as shown before, the position signals maintain the same shape for the three cases (see figure 4).

Figure 14 shows the amplitude of the FFT of the axis 3 position signal (case *i* and case *iii*). The spectrum is also approximated by trendlines in a frequency range larger than one decade. Here the trendlines present slopes that vary slightly (slope  $m = -2.54$  for case *i* and slope  $m = -2.50$  for case *iii*). The study of the case *ii*) presents a trendline with a slope of  $m = -2.62$ . Therefore, the lines present, clearly, fractional order behavior in all cases.

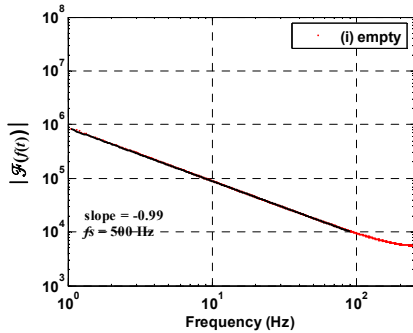


Figure 13. Spectrum of the axis 1 position for the trapezoidal profile

The others position signals (axis 2 and 4) were studied, revealing also a well defined spectrum. Their trendlines present middle slope values that are difficult to classify in terms of its behavior as fractional or integer order. In what concerns to the axis 5 position signal, as it maintains the same value during all time acquisition, it consists only in a direct current component.

Figure 15 shows, as an example, the FFT amplitude of the electrical current for the motor axis 3, that occurs in the case of the trapezoidal profile with container carrying a liquid (case *iii*). A trendline with slope  $m = -1.19$  is calculated in a frequency range larger than one decade and superimposed to the signal. The others current signals were studied, revealing also an identical behavior in terms of its spectrum spread, for the tested conditions (cases *i*, *ii* and *iii*).

According to the robot manufacturer specifications the loop control of the robot has a cycle time of  $t_c = 10$  ms. This fact is observed approximately at the fundamental

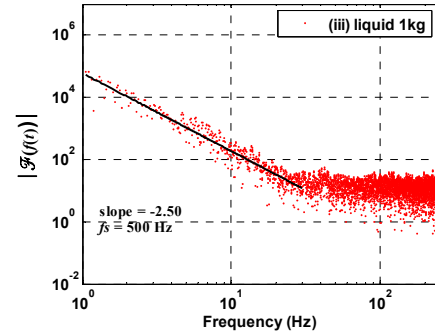
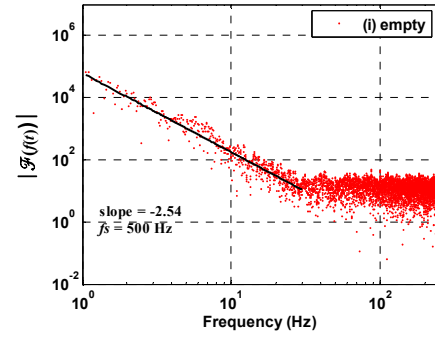


Figure 14. Spectrum of the axis 3 position for the trapezoidal profile

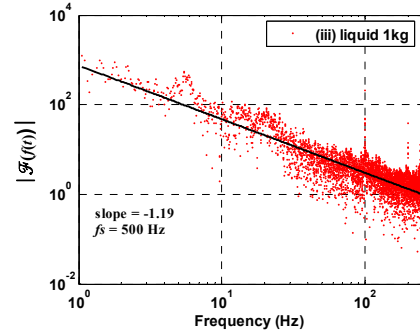


Figure 15. Spectrum of the axis 3 motor current for the trapezoidal profile

( $f_c = 100$  Hz) and multiple harmonics in all spectra of motor currents (figure 15).

Figure 16 shows the FFT amplitude of the  $F_x$  force (case *i*) for the trapezoidal profile. A trendline with slope  $m = -2.52$  is calculated in a frequency range larger than one decade and superimposed to the signal.

Figure 17 shows the FFT amplitude of the  $F_y$  force (cases *i* and *iii*) for the trapezoidal profile. Two trendlines with slopes  $m = -2.49$  and  $m = -2.53$ , for the cases *i*) and *iii*), were calculated in a frequency range larger than one decade and superimposed to the signal. The slope values of the force components presented (figures 16 and 17) show a fractional order behavior. In general, the forces for the other cases not shown have a spectrum that can be approximated by a trendline in a frequency range greater than one decade. Their trendlines present middle slope values that are difficult to classify in terms of its behavior as fractional or integer order.

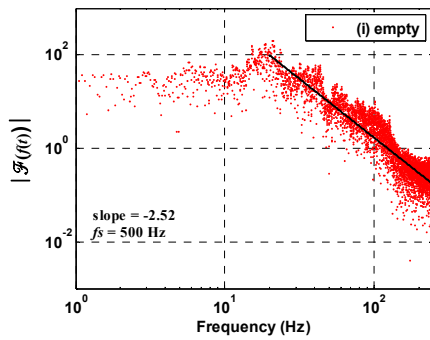


Figure 16. Spectrum of the  $F_x$  force for the trapezoidal profile

Figure 18 shows the FFT amplitude of the  $M_z$  moment (case *ii*) for the trapezoidal profile. This spectrum has not defined a clear pattern in a large frequency range. Moreover, all moments spectra present identical behavior. Therefore, it is difficult to define accurately the behavior of signals in terms of integer or fractional dynamics.

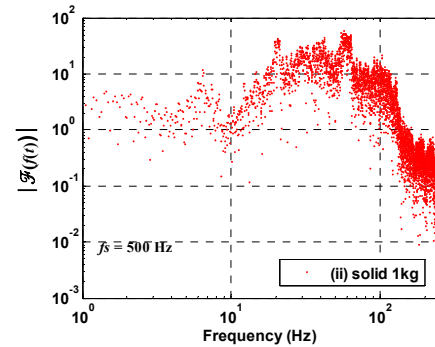


Figure 18. Spectrum of the  $M_z$  moment for the trapezoidal profile

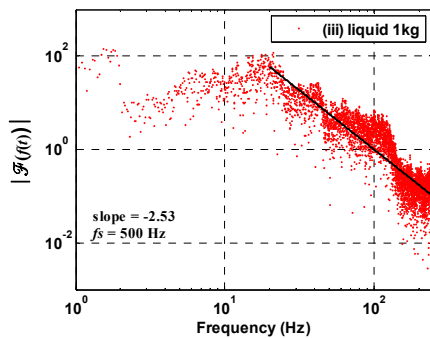
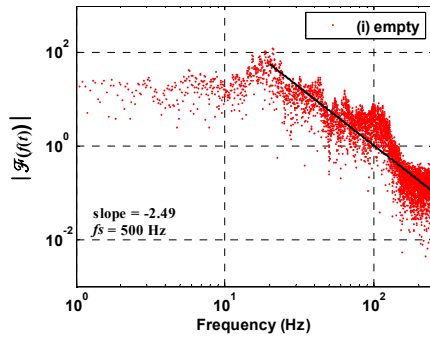


Figure 17. Spectrum of the  $F_y$  force for the trapezoidal profile

Finally, figure 19 depicts the spectrum of the signal captured from the accelerometer 1 located at the container. Like the spectrum from the other accelerometer, this spectrum is spread and complicated. Therefore, it is difficult to define accurately the slope of the signal and, consequently, its behavior in terms of integer or fractional dynamics.

The spectra of the signals for the trapezoidal profile were studied in terms of their integer *versus* fractional behavior. The spectra for the parabolic profile were also analyzed, but

due to space limitations are not presented here. The signals in time domain for the parabolic profile present a smoother dynamics, when compared with those of the trapezoidal profile. Nevertheless, both cases reveal identical behavior in terms of integer *versus* fractional characteristics.

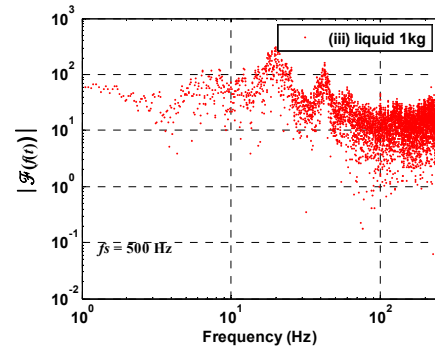


Figure 19. Acceleration spectrum of the container for the trapezoidal profile

### Windowed Fourier Transform:

Several spectra of the signals captured during approximately 20 seconds are represented in figures 13–19. For the most part of the signals their spectra are scattered and, therefore, in order to obtain smoother curves a multiwindow algorithm can be used. If we time slice the signals and calculate the Fourier transform, then, for each section of the signal, the resulting spectrum is a smoother curve. One way of obtaining the time-dependent frequency content of a signal is to take the Fourier transform of a function over an interval around an instant  $\tau$ , where  $\tau$  is a variable parameter [15]. The Gabor Transform accomplishes this by using the Gaussian window. The windowed Fourier transform (WFT), also known as short time Fourier transform (STFT), generalizes the Gabor transform by allowing a general window function [20]. The concept of this mathematical tool is very simple. We multiply the signal to be analyzed  $x(t)$ , by an analysis moving window  $g(t-\tau)$ , and then we compute the Fourier transform of the windowed signal  $x(t)g(t-\tau)$ . Each FT gives a frequency domain ‘slice’ associated with the time value at the window centre. Actually, windowing the signal improves local spectral

estimates [20]. Considering the window function centered at time  $\tau$ , the WFT is represented analytically by:

$$F_w(\tau, \omega) = \int_{-\infty}^{+\infty} x(t)g(t-\tau)e^{-j\omega t} dt \quad (2)$$

where  $\omega = 2\pi f$  is the frequency.

Each window has a width  $t_w$  and the distance between two consecutive windows can be defined in a way so that they become overlapped during a percentage of time  $\beta$  in relation with  $t_w$ . Therefore, the frequencies of the analyzing signal  $f < 1/t_w$  are rejected by the WFT. Diminishing  $t_w$  produces a reduction of the frequency resolution and an increase in the time resolution. Augmenting  $t_w$  has the opposite effect. Therefore, the choice of the WFT window entails a well-known duration-bandwidth tradeoff.

On the other hand, the window can introduce an unwanted side effect in the frequency domain. As a result of having abrupt truncations at the ends of the time domain caused by the window, specially the rectangular one, the spectrum of the FT will include unwanted "side lobes". This gives rise to an oscillatory behavior in the FT results called the Gibbs Phenomenon [21]. In order to reduce this unwanted effect, generally is used a weighting window function that attenuate signals at their discontinuities. For that reason there are several others popular windows normally adopted in the WFT as, for example, Hanning, Hamming, Gaussian and Blackman [18].

If the windows do not overlap, then it is clear that some data are lost. On the other hand, if the windows overlap in a short period of time a significant part of the time signal is ignored due to the fact that most windows exhibit small values near the boundaries. To avoid this loss of data, overlap analysis must be performed.

As analyzed previously for the FT, in order to study the behavior of each  $F_w(\tau, \omega)$ , a trendline with slope  $m_i$  is now superimposed over the spectrum during, at least, one decade. Having these ideas in mind is possible to relate the slope  $m$ , of the FT's trendline, with the set of slope  $m_i$  of the WFT's trendlines. In fact the slope  $m$  of the trendline superimposed over the FT can be seen heuristically as a weighted average of the slopes  $m_i$  of the WFT trendlines obtained for the  $n$  windows:

$$m_{av} \sim \frac{\sum_{i=1}^n a_i m_i}{\sum_{i=1}^n a_i} \quad (3)$$

where the weight  $a_i$  is the signal's energy for each  $i$ th WFT window ( $i = 1, \dots, n$ ).

The practice reveals that this heuristic formula is suitable when the trendline fits well in the numerical data.

In this line of thought, the spectra of the signals approximated by trendlines, are analyzed with the WFT. Due to space limitations we are only depicting the more relevant features. In the study presented a Gaussian window was adopted according to the expression:

$$g(t) = e^{-\frac{1}{2}\left(\alpha \frac{t}{t_w/2}\right)^2} \quad (4)$$

where the parameter  $\alpha = 2.5$  and  $t_w$  is the width of the window.

The value for the Gaussian window overlap is  $\beta = 50\%$  and the window's width is  $t_w = 2$  s. The standard trial and error procedure was used to find the suitable windows overlap.

Figure 20 a) depicts the axis 3 motor current for the trapezoidal profile (case *iii*). Figure 20 b) shows its spectrum

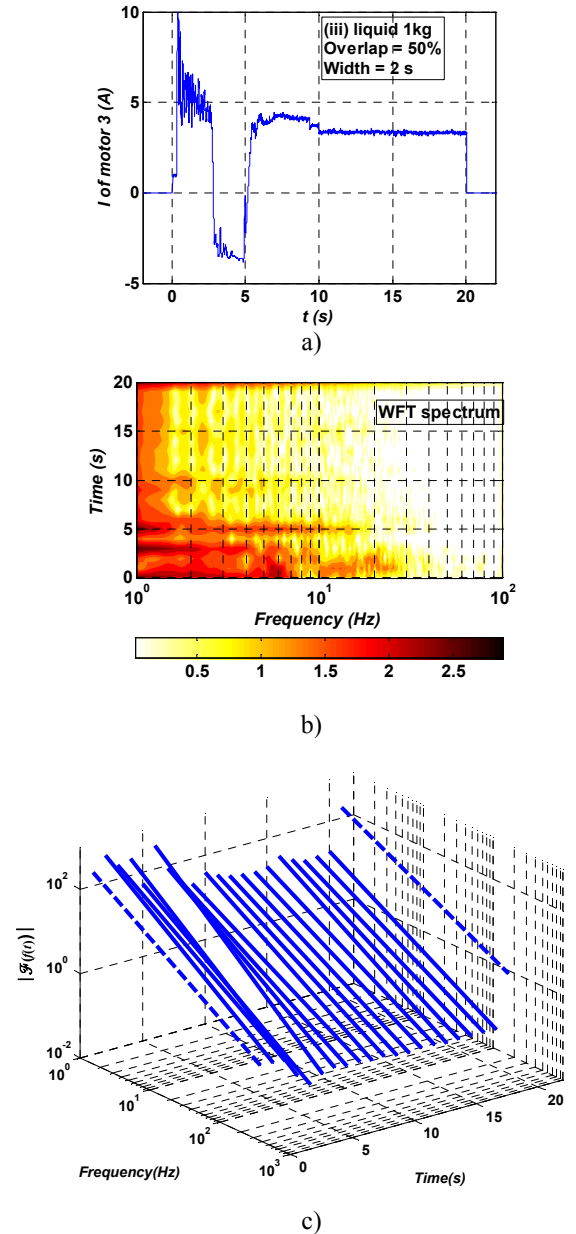
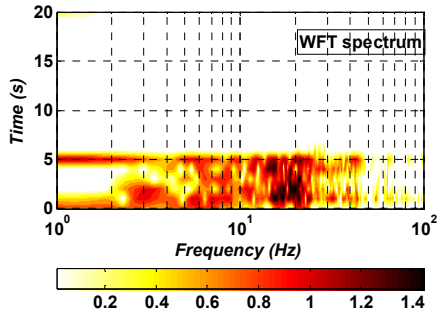
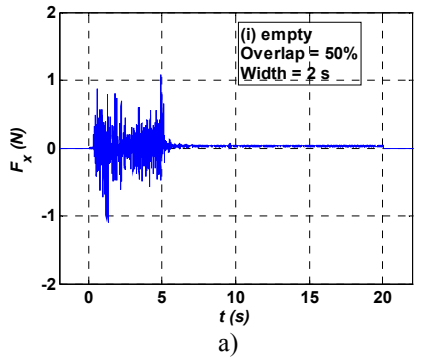
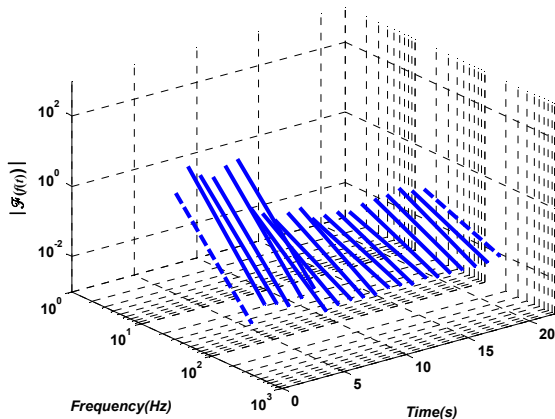


Figure 20. WFT of the axis 3 motor current for the trapezoidal profile

along the time obtained with the WFT. According with the approach used before, a trendline was calculated between frequencies  $1 < f < 250$  Hz for the spectrum obtained with each moving window. The set of resulting trendlines are shown on figure 20 c). The trendlines for the windows centered approximately at time  $\tau = 0$  s and  $\tau = 20$  s (dashed lines) present a distinct behavior as a result of the signal having abrupt truncations at the ends of the time. This fact can be partial observed also in figure 20 b). Here the spectrum presents a considerable energy for frequencies  $1 < f < 100$  Hz at  $\tau = 20$  s due to the discontinuities of the signal in time. In consequence we do not consider those trendlines in our study.



b)

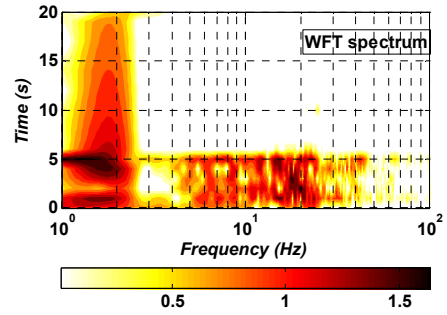
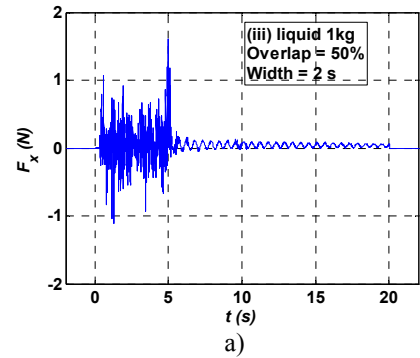


c)

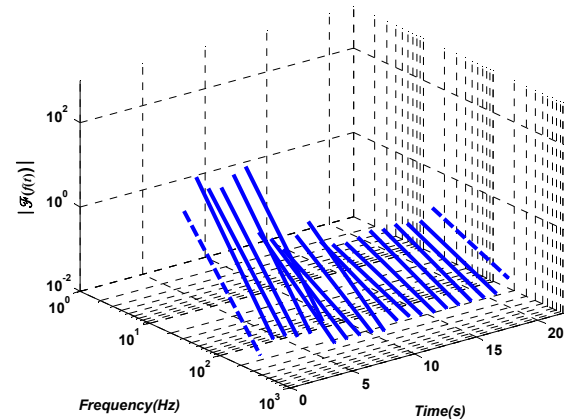
Figure 21. WFT of the  $F_y$  force for the trapezoidal profile case *i*)

The slope values of the solid trendlines shown in figure 20 c) varies between  $-1.49 < m < -0.97$ . Using (3) the equivalent slope value obtained is  $m_{av} = -1.16$ , which is close to the trendline slope value  $m = -1.19$  of the FT calculated over de same range of frequencies  $1 < f < 250$  Hz (figure 15).

Figure 21 presents a set of signals related with the WFT of the  $F_y$  force for the trapezoidal profile case *i*). The slope values of the solid trendlines shown in figure 21 c) varies between  $-2.68 < m < -0.80$ . Using the heuristic expression (3) the obtained equivalent slope is  $m_{av} = -2.47$ , which value is again close to the slope value  $m = -2.49$  of the FT trendline superimposed over de same range of frequencies  $20 < f < 250$  Hz (figure 17 case *i*).



b)



c)

Figure 22. WFT of the  $F_y$  force for the trapezoidal profile case *iii*)

Finally, figure 22 depicts a set of signals related with the WFT of the  $F_y$  force for the trapezoidal profile case *iii*). The oscillation of the signal in time domain (figure 22 a) reveals the effect of the liquid slosh during the acquisition time of 20 s. This fact is observed in figure 22 b) where the energy of the spectrum, for approximately  $1 < f < 2.5$  Hz, reveals a significant value. The solid trendlines shown in figure 22 c) varies between  $-2.74 < m < -0.80$ . Using (3) the equivalent slope value obtained is  $m_{av} = -2.45$ . Again this value is close to the slope value  $m = -2.53$  of the FT trendline superimposed over de same range of frequencies (figure 17 case *iii*).

## CONCLUSIONS

In this paper an experimental study was conducted to investigate several robot signals during the motion of a liquid

container. The amount of slosh depends, among other aspects, on how the container is accelerated. In order to test different acceleration shapes two types of trajectory velocity were used: the trapezoidal and the parabolic profiles. Although the signals in time domain present different dynamics for the two profiles, their spectra reveals identical behavior in terms of integer *versus* fractional characteristics. The study was conducted in a fractional system perspective and provides useful information that can assist in the design of a control system to be used in reducing or eliminating the effect of vibrations.

In future work, we plan to pursue several research directions to help us further understand the behavior of the signals.

## REFERENCES

- [1] Singer, N. C. and W. P. Seering. Using Acausal Shaping Techniques to Reduce Robot Vibration. Proc. IEEE Int. Conf. on Robotics and Automation. Philadelphia PA., April 25-29, 1988.
- [2] Yoshikawa, T., K. Hosoda, T. Doi and H. Murakami. Quasi-static Trajectory Tracking Control of Flexible Manipulator by Macro-micro Manipulator System, Proc. IEEE Int. Conf. on Robotics and Automation, pp. 210-215, 1993.
- [3] Magee, David P. and Wayne J. Book. Filtering Micro-Manipulator Wrist Commands to Prevent Flexible Base Motion. Proc. American Control Conf., Seattle, Washington, June, 1995.
- [4] Cannon, David W., David P. Magee and Wayne J. Book, Jae Y. Lew. Experimental Study on Micro/Macro Manipulator Vibration Control. Proc. IEEE Int. Conf. on Robotics and Automation. Minneapolis, Minnesota, April, 1996.
- [5] Lew, J.Y., Trudnowski, D. J., Evans, M. S., and Bennett, D. W. Micro-Manipulator Motion Control to Suppress Macro-Manipulator Structural Vibrations. Proc. IEEE Int. Conf. on Robotics and Automation, Vol. 3, pp. 3116-3120, 1995.
- [6] Machado, J. A. Tenreiro. Analysis and Design of Fractional-Order Digital Control Systems, Journal Systems Analysis-Modelling-Simulation, Gordon & Breach Science Publishers, vol. 27, pp. 107-122, 1997.
- [7] Machado, J. A. Tenreiro. A Probabilistic Interpretation of the Fractional-Order Differentiation, Journal of Fractional Calculus & Applied Analysis, vol. 6, No 1, pp. 73-80, 2003.
- [8] Podlubny, I. Geometrical and physical interpretation of fractional integration and fractional differentiation. Journal of Fractional Calculus & Applied Analysis, vol. 5, No 4, pp. 357-366, 2002.
- [9] Bohannan, Gary W. Analog Realization of a Fractional Control Element -Revisited [mechatronics.ece.usu.edu/foc/cdc02tw/cdrom/aditional/FOC\\_Proposal\\_Bohannan.pdf](http://mechatronics.ece.usu.edu/foc/cdc02tw/cdrom/aditional/FOC_Proposal_Bohannan.pdf), 2002.
- [10] Barbosa, Ramiro S., J. A. Tenreiro Machado and Isabel M Ferreira. Tuning of PID Controllers Based on Bode's Ideal Transfer Function, Nonlinear Dynamics 38: pp. 305-321, Kluwer Academic Publishers, 2004.
- [11] Oustaloup, Alain, Xavier Moreau and Michel Nouillant. From fractal robustness to non integer approach in vibration insulation: the CRONE suspension, Proceedings of the 36th Conference on Decision & Control, San Diego, California, USA, December, 1997.
- [12] Lima, Miguel F. M., J.A. Tenreiro Machado, and Manuel Crisóstomo. Experimental Set-Up for Vibration and Impact Analysis in Robotics, WSEAS Trans. on Systems, Issue 5, vol. 4, May, pp. 569-576, 2005.
- [13] Lima, Miguel F. M., J.A. Tenreiro Machado, and Manuel Crisóstomo. Fractional Order Fourier Spectra In Robotic Manipulators With Vibrations, Second IFAC Workshop on Fractional Differentiation and its Applications, Porto, Portugal. 2006.
- [14] Lima, Miguel F. M., J.A. Tenreiro Machado, and Manuel Crisóstomo. Windowed Fourier transform of experimental robotic signals with fractional behavior. In Proc. IEEE Int. Conf. on Computational Cybernetics, pages 21-26, Tallin, Estonia, August, 2006.
- [15] D. Gabor. Theory of communication. J. IEE 1946.
- [16] Grundelius, M.. Methods for Control of Liquid Slosh. PhD thesis, Lund Institute of Technology, Sweden, October 2001.
- [17] Feddema, J.T., C.R. Dohrmann, G.G. Parker, R.D. Robinett, V.J. Romero, and D.J. Schmitt. Control for slosh-free motion of an open container. IEEE Control Systems, 17(1):29-36, February 1997.
- [18] Harris, Fredric J., On the Use of Windows for Harmonic Analysis with the Discrete Fourier Transform. Proc. IEEE, vol. 66, n. 1, January 1978.
- [19] Lima, Miguel F. M., J.A. Tenreiro Machado, and Manuel Crisóstomo. Fractional Dynamics in Mechanical Manipulation, Accepted for the ASME 2007 Int. Design Engineering Technical Conf. & Computers and Information in Engineering Conf., September 4-7, 2007, Las Vegas, Nevada, USA.
- [20] Ronald L. Allen, Duncan W. Mills, Signal Analysis, IEEE Press, Wiley-Interscience, 2004.
- [21] Alan V. Oppenheim, Ronald W. Schaffer, John R. Buck, Discrete-Time Signal Processing, 2nd Edition, Prentice Hall, 1989.
- [22] Vasily E. Tarasov and George M. Zaslavsky, Fractional dynamics of systems with long-range interaction, Communications in Nonlinear Science and Numerical Simulation, Volume 11, Issue 8, December 2006, Pages 885-898.
- [23] Nickolay Korabel, George M. Zaslavsky and Vasily E. Tarasov, Coupled oscillators with power-law interaction and their fractional dynamics analogues, Communications in Nonlinear Science and Numerical Simulation, Volume 12, Issue 8, December 2007, Pages 1405-1417.
- [24] Vasily E. Tarasov and George M. Zaslavsky, Conservation laws and Hamilton's equations for systems with long-range interaction and memory, Communications in Nonlinear Science and Numerical Simulation, In Press, Corrected Proof, Available online 24 May 2007, doi:10.1016/j.cnsns.2007.05.017.
- [25] Maria da Graça Marcos, Fernando B.M. Duarte and J.A. Tenreiro Machado, Fractional dynamics in the trajectory control of redundant manipulators Communications in Nonlinear Science and Numerical Simulation, In Press, Corrected Proof, Available online 16 April 2007, doi:10.1016/j.cnsns.2007.03.027.